

## ORIGINAL ARTICLE

# Feasibility of Patient-Specific Quality Assurance Using Gamma Analysis for IMRT Plans in Laryngeal Cancer

Mohammad Javad Enferadi-Aliabad<sup>1\*</sup> , Mohammad Ali Broomand<sup>2</sup>, Abolfazl Nikfarjam<sup>1</sup>

<sup>1</sup> Department of Medical Physics, School of Medicine, Shahid Sadoughi University of Medical Sciences, Yazd, Iran

<sup>2</sup> Department of Radiotherapy, School of Medicine, Shahid Sadoughi University of Medical Sciences, Yazd, Iran

\*Corresponding Author: Mohammad Javad Enferadi-Aliabad

Received: 30 November 2024 / Accepted: 11 February 2025

Email: [enferadiimj@gmail.com](mailto:enferadiimj@gmail.com)

## Abstract

**Purpose:** Laryngeal cancer is a critical health issue, often treated using advanced radiation therapy techniques such as Intensity-Modulated Radiation Therapy (IMRT). The gamma index is a widely used metric for quality assurance in radiotherapy, assessing the agreement between planned and delivered dose distributions.

This study aims to evaluate the feasibility and accuracy of laryngeal IMRT treatment plans using three gamma analysis algorithms and varying evaluation parameters, including Dose Difference (DD%), and Distance-To-Agreement (DTA).

**Materials and Methods:** IMRT treatment plans for laryngeal cancer were generated using the Prowess Panther V5.5 Treatment Planning System (TPS). Patient-Specific Quality Assurance (PSQA) was conducted using EBT3 Gafchromic films scanned at 350 dpi and analyzed with RIT Complete 6.11 software. Dose distributions were evaluated using three gamma analysis algorithms under 3%/3 mm criteria and low-dose thresholds of 15%. Calibration of the films was performed to ensure accurate dose measurements.

**Results:** Gamma Passing Rates (GPR) for the laryngeal IMRT plans demonstrated high accuracy, with over 90% of pixels passing the criteria in most cases. Composite gamma analysis showed 53.89% of pixels meeting both DD and DTA criteria simultaneously, while individual evaluation revealed the impact of stricter thresholds on GPR. Subtraction analysis identified dose discrepancies, emphasizing the need for accurate calibration.

**Conclusion:** This study highlights the effectiveness of gamma analysis in ensuring the accuracy of IMRT treatment plans for laryngeal cancer. The findings underscore the importance of rigorous PSQA, parameter optimization, and advanced algorithms to enhance treatment precision.

**Keywords:** Laryngeal Cancer; Intensity-Modulated Radiation Therapy; Gamma Analysis; EBT3 Film; Patient-Specific Quality Assurance; Radiotherapy.

## 1. Introduction

Laryngeal cancer is a notable subset of head and neck malignancies, accounting for approximately 185,000 new cases worldwide annually with substantial mortality rates remaining a global concern [1, 2]. The disease predominantly affects men, with a male-to-female ratio of about 6:1, and is strongly linked to risk factors such as tobacco and alcohol consumption [2]. Advances in modern oncology have positioned radiation therapy as a critical modality for managing laryngeal cancer enabling effective tumor control while preserving vital anatomical and functional structures [3]. Among these advancements, Intensity-Modulated Radiation Therapy (IMRT) has emerged as a transformative approach delivering precise and conformal dose distributions to the target region while minimizing exposure to surrounding healthy tissues [4].

The precision of IMRT arises from its ability to modulate beam intensity dynamically through advanced systems such as Multileaf Collimators (MLCs) [5, 6]. This complexity, however, introduces potential uncertainties stemming from factors such as beam modeling errors, patient movement, organ motion, and setup inaccuracies [7]. To mitigate these challenges and ensure treatment accuracy, robust Patient-Specific Quality Assurance (PSQA) protocols are essential [8]. These protocols verify that the planned dose distributions are faithfully delivered during treatment.

One of the most widely utilized PSQA methodologies is gamma analysis, introduced by Low *et al.* [9]. This technique evaluates the agreement between measured and calculated dose distributions by combining two critical criteria Dose Difference (DD) and Distance-To-Agreement (DTA) into a single metric. For each reference point, the gamma value is calculated as (Equations 1, 2):

$$\Gamma(\vec{r}_C, \vec{r}_m) = \sqrt{\frac{|\vec{r}_C - \vec{r}_m|^2}{DTA^2} + \frac{|D(\vec{r}_m) - D(\vec{r}_C)|^2}{\Delta D^2}} \quad (1)$$

$$\gamma(\vec{r}_C, \vec{r}_m) = \min\{\Gamma(\vec{r}_C, \vec{r}_m)\} \forall \{\vec{r}_m\} \quad (2)$$

Despite the widespread use of gamma analysis, variations in its implementation, including

normalization methods and threshold settings, can significantly impact the Gamma Passing Rate (GPR). These variations necessitate detailed investigations to optimize gamma parameters and improve the reliability of QA procedures.

Numerous studies have examined the reliability of gamma analysis in radiotherapy quality assurance, focusing on its application in evaluating treatment plan accuracy. For instance, Coleman *et al.* (2013) investigated the impact of MLC positional errors on gamma passing rates, demonstrating that stricter gamma criteria, such as 2%/2 mm, yield higher sensitivity in detecting treatment delivery inaccuracies [10]. Similarly, Song *et al.* (2015) explored the role of low-dose thresholds in gamma analysis, highlighting their influence on GPR outcomes [11]. These studies emphasize the importance of optimizing gamma evaluation parameters to enhance the accuracy and clinical relevance of dose delivery validation, which aligns with the goals of this study in assessing IMRT treatment plans.

This study aims to evaluate the accuracy of laryngeal cancer IMRT treatment plans using three gamma analysis algorithms at Shahid Ramezan-Zadeh Radiation Oncology Center in Yazd.

## 2. Materials and Methods

A CT dataset from a laryngeal cancer case was used. The CT scan was contoured by a radiation oncologist to delineate the Clinical Target Volume (CTV) and Organs At Risk (OARs) according to standard guidelines. A step-and-shoot Siemens ONCOR IMRT technique was employed to create the treatment plan, consisting of nine beams arranged at equal gantry angle intervals of 40 degrees. Each beam included nine subfields optimized to deliver a prescription dose of 200 cGy per fraction. The treatment plan was calculated using Prowess Panther V5.5 and exported for further validation.

To verify dose distributions, an acrylic Universal IMRT Verification Phantom made of water-equivalent material was used. The treatment plan was mapped onto the phantom's CT dataset to replicate the treatment delivery. An ionization chamber, PTW Semiflex Chamber (0.125 cm<sup>3</sup>) was utilized to

perform point dose measurements at specific locations in the phantom (Figure 1).

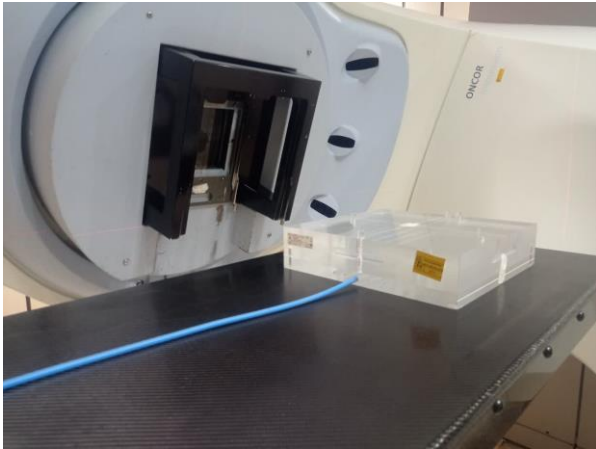


**Figure 1.** Dose difference test performed on the universal phantom

Gafchromic EBT3 films (Ashland, USA) were employed to measure two-dimensional dose distributions. Before initiating film dosimetry, point dose measurements were conducted to confirm the accuracy of the treatment delivery system (Figure 2). These measurements were performed using an ionization chamber placed at predefined points within the phantom. The measured absorbed doses at these points were compared to the calculated doses from the TPS. After point dose measurements the films were carefully cut to appropriate sizes ( $4 \times 4 \text{ cm}^2$ ) and positioned within the phantom at the target regions. After irradiation, the films were scanned using a flatbed scanner Microtek 9800xl in all-channel mode at a resolution of 350 dpi. Pixel values from the scanned images were converted into absolute dose values using a pre-established calibration curve.

The gamma index was employed to evaluate the agreement between measured and calculated dose distributions using three different algorithms: Low *et al.* (1998), Ju *et al.* [12], and a third algorithm incorporating advanced filtering techniques [13]. Each algorithm offered unique advantages for analyzing dose accuracy. The Low *et al.* algorithm, widely regarded as the standard, evaluates DD and DTA criteria with a balance of precision and computational efficiency. The Ju *et al.* algorithm employs a geometric approach for gamma index calculation, avoiding conventional interpolation methods. It divides the evaluated dose distribution into simpler geometric units (e.g., triangles in 2D and tetrahedrons

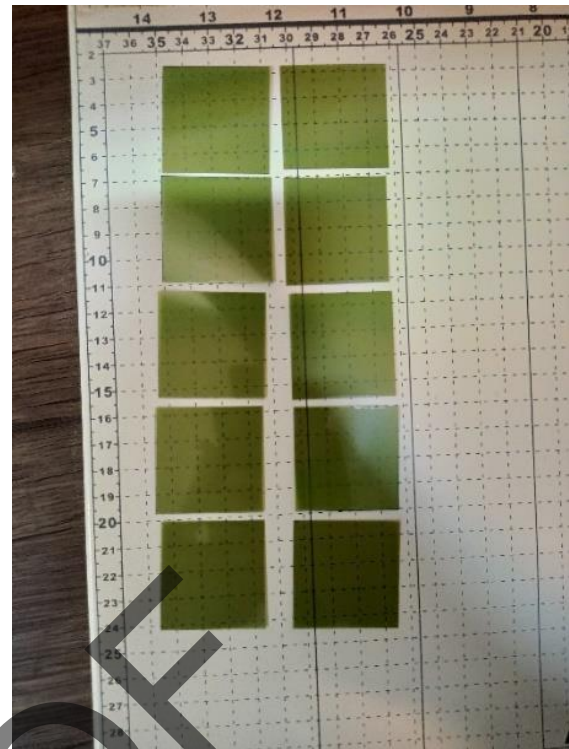


**Figure 2.** Gafchromic EBT3 film slices ( $4 \times 4 \text{ cm}$ ) prepared for dose calibration

in 3D) and calculates the shortest distance between the reference and evaluated distributions algebraically. This method significantly reduces computation time while maintaining accuracy, making it efficient for high-resolution dose distributions. The filtering algorithm for gamma index calculation employs a multi-level approach to enhance efficiency and accuracy. In the first level, a search region around each reference point identifies potential matches with minimal computations. If no match is found, the second level uses dose difference signs to infer a match. The third level conducts precise interpolation along the boundaries to ensure no potential match is overlooked, particularly in areas with gradual dose gradients.

The analysis was conducted under standard evaluation parameters, including a DD of 3%, DTA of 3 mm, and a low-dose threshold of 15%. Additionally, the sensitivity of gamma passing rates to variations in DD, DTA was systematically examined across all three algorithms.

Gamma calculations were performed using RIT Complete 6.11 software. Results were reported as gamma passing rates, representing the percentage of pixels with gamma values  $\leq 1$ .

### 3. Results

#### 3.1. Film Calibration and Point Dose Verification

The percentage dose difference for all evaluated points was found to be less than 3%, indicating precise calibration of the treatment machine and TPS agreement. This step ensured that subsequent film dosimetry results would be meaningful and reliable (Table 1).

**Table 1.** Percentage dose differences measured using the ionization chamber compared to the treatment planning system for film calibration

Plan	Dose Reported in TPS	Dose Measure with Ion chamber	Dose Difference(%)
10	9.51	9.66	-1.67%
30	28.54	29.25	-2.65%
60	57.08	57.8	-1.47%
80	76.1	76.6	-0.69%
100	95.13	96.3	-1.24%
120	114.15	115.8	-1.59%
140	133.18	135.6	-1.86%
190	180.75	183.9	-2.15%
220	206.62	213.2	-3.18%
240	228.32	232.6	-1.88%
290	275.88	208.7	-1.78%
350	333.44	338.3	-1.46%
400	380.53	385.8	-1.39%

Following point dose verification, the gafchromic EBT3 films were placed within the Universal phantom to capture dose distributions. A third-degree polynomial function was applied to establish the relationship between the pixel values and absolute dose levels, with an  $R^2$  value exceeding 0.92. The calibration plot of the film shows that the behavior of gafchromic EBT3 films exhibits linearity in the dose range of 0 to 400 cGy, and as the dose increases, the pixel value decreases (Figure 3).

The treatment plan was designed with monitor units for the beams ranging from 45.2 to 68.3. The reference image center was at [90.89, 104.59] mm, and the target image center was at [90.39, 103.42] mm, resulting in deviations of 0.49 mm on the x-axis and 1.16 mm on the y-axis, demonstrating precise isocenter alignment. The figure below illustrates the dose distribution of the IMRT plan for this patient (Figure 4).

The gamma index was calculated under standard conditions (3% dose difference/3 mm distance to agreement) using the algorithm proposed by Low *et al.* and normalization to the maximum image value. Gamma analysis results showed a total of 26,543 pixels, of which 1,250 pixels (4.71%) had gamma values greater than 1, and 25,293 pixels (95.29%) had gamma values less than or equal to 1. The maximum gamma value was 2.70, the minimum was 0.00, the mean was 0.47, and the standard deviation was 0.27. The DTA search radius was set at 10 mm (Figures 5, 6).

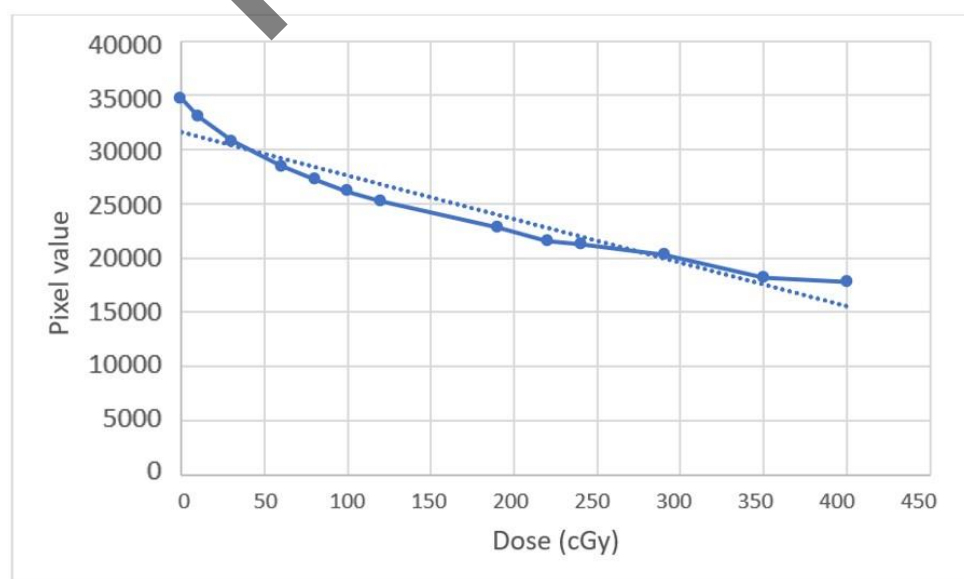


**Figure 3.** Calibration curve of radiochromic films in the dose range of 0 to 400 cGy



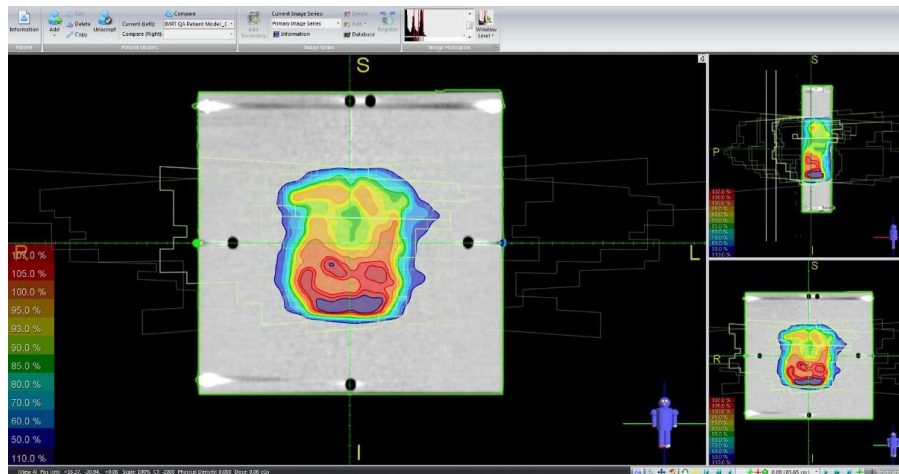


**Figure 4.** Dose distribution of the laryngeal IMRT plan mapped onto CT images of the universal phantom

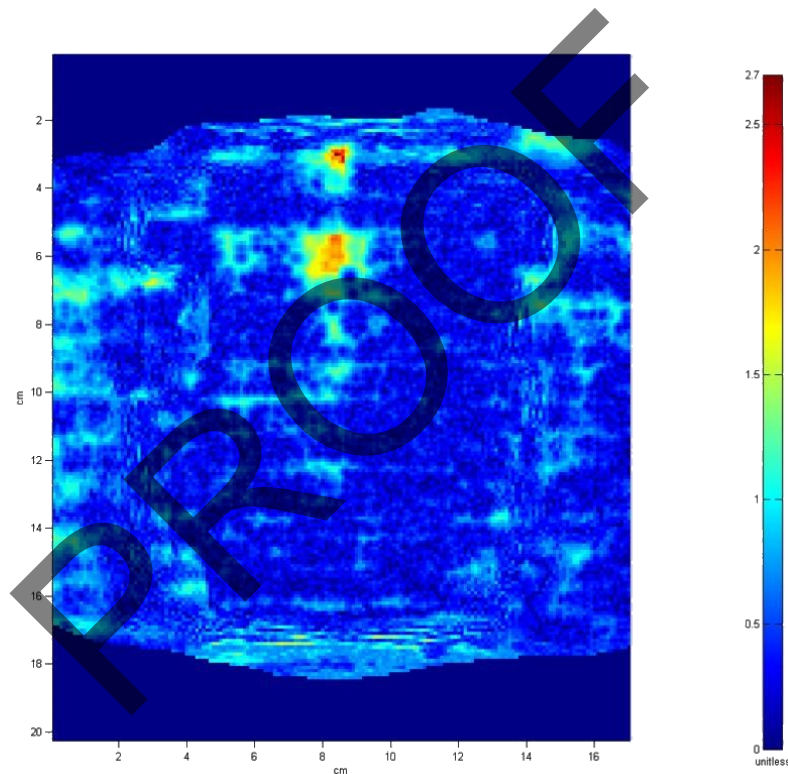


**Figure 5.** Gamma analysis of the laryngeal IMRT plan

### 3.2. Profile Analysis

Vertical and horizontal dose profiles were evaluated at predefined positions. The vertical profile showed that approximately 50% of pixels were within the  $\pm 3\%$  dose difference tolerance, indicating moderate agreement in this axis. Conversely, the horizontal profile showed improved results, with over 70% of pixels within the same tolerance, reflecting a better dose agreement in the horizontal direction. The

maximum observed dose difference in the vertical profile was 7.04%, while the minimum was  $-15.50\%$ . For the horizontal profile, the maximum deviation was 8.27%, and the minimum was  $-6.93\%$  (Figures 7, 8).

### 3.3. Subtraction Analysis

In the subtraction analysis, the mean dose difference was calculated as  $-1.74\%$ , with a standard deviation of 3.58%. The analysis revealed that 57.87% of the pixels were within the 3% dose difference

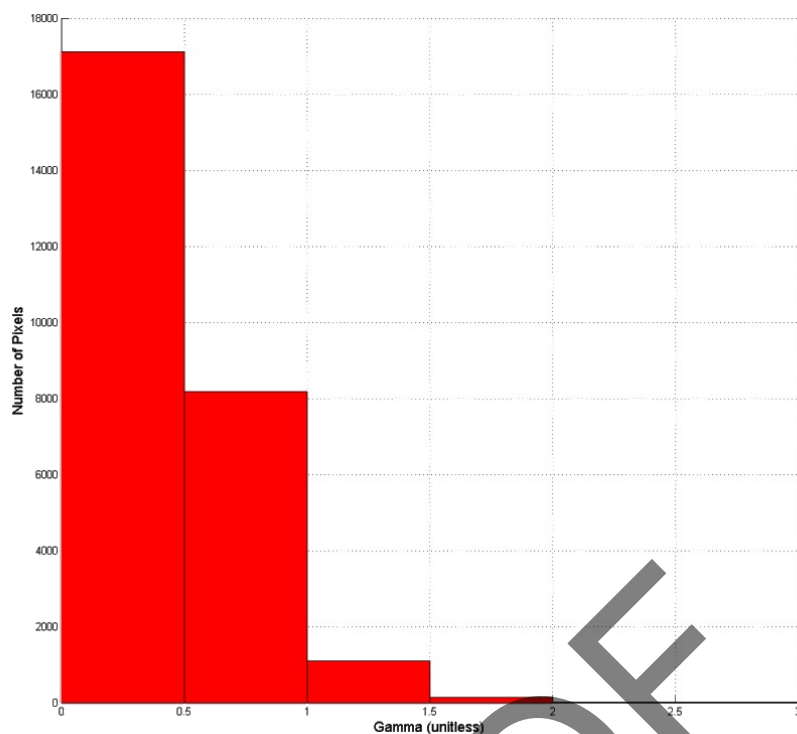


**Figure 6.** Histogram of gamma analysis for the laryngeal IMRT plan

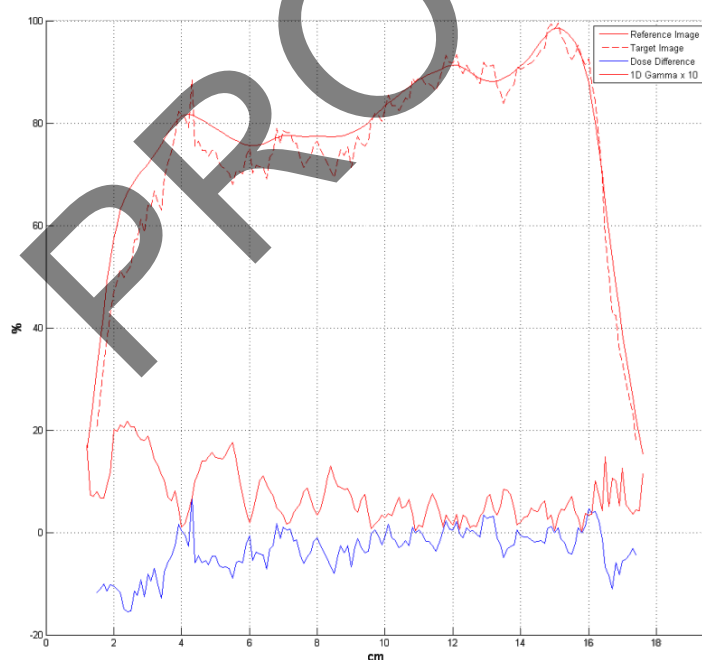


**Figure 7.** Vertical profile analysis of the laryngeal IMRT plan

tolerance, confirming a reasonable level of agreement but suggesting space for improvement in low-dose regions. The subtraction proportion passing plot demonstrates the proportion of pixels meeting the tolerance levels based on pixel-by-pixel subtraction of the target and reference dose distributions. The

relative area under the subtraction curve is measured as 0.692, while the fine-tuned subtraction curve has a relative area of 0.679, indicating slight variations in dose agreement across the total of 26,985 analyzed pixels (Figure 9).

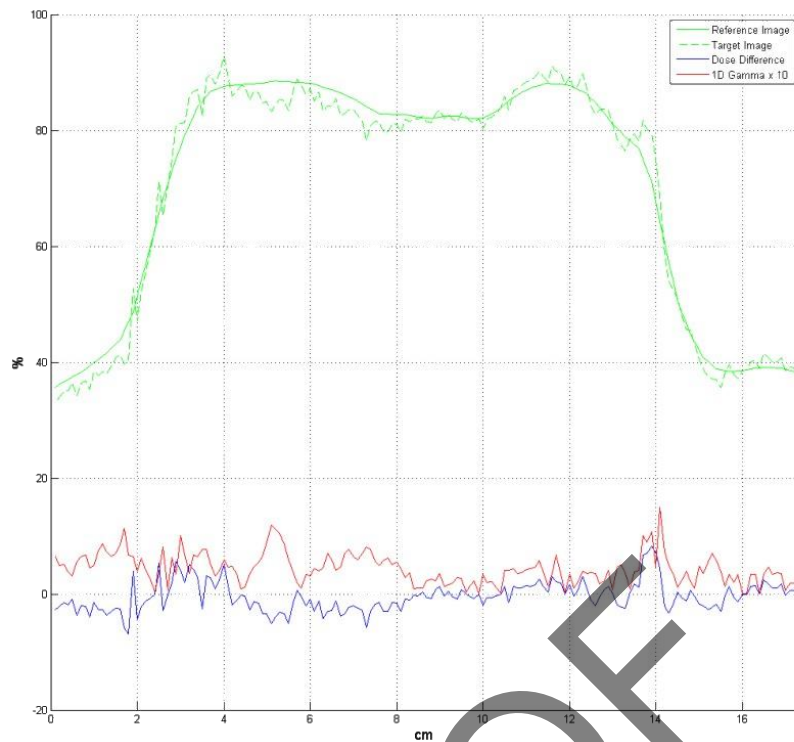


**Figure 8.** Horizontal profile analysis of the laryngeal IMRT plan

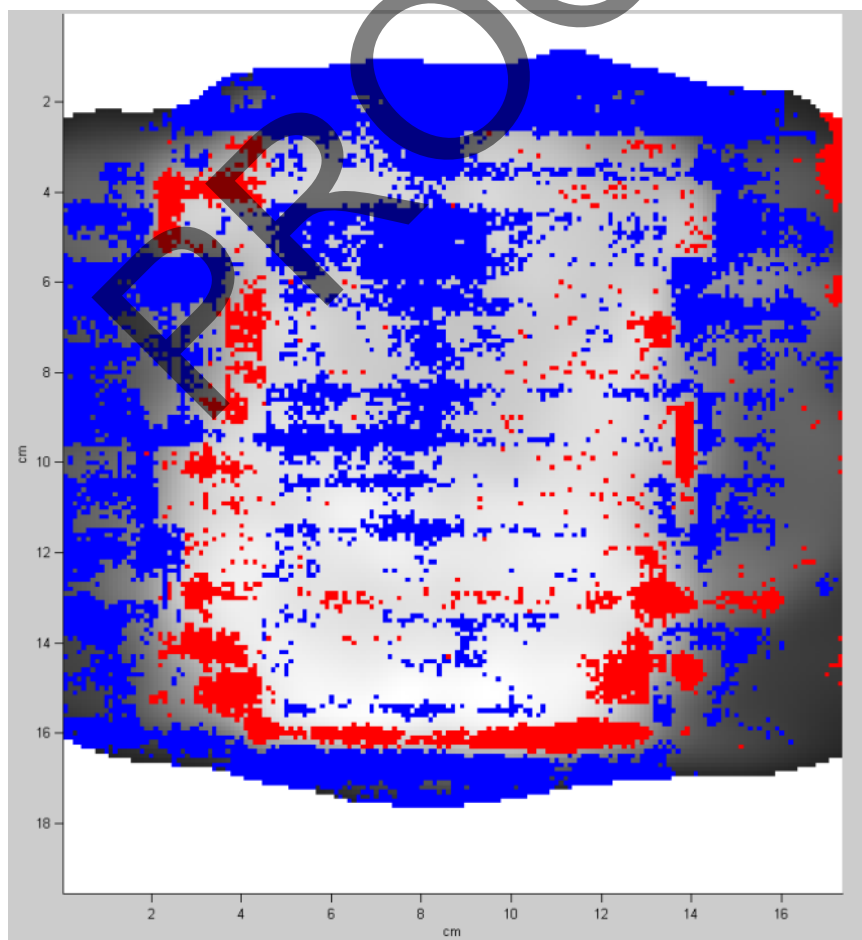


**Figure 9.** Subtraction analysis of the laryngeal IMRT plan

### 3.4. Composite Analysis

Composite analysis was performed, evaluating 26,985 pixels in total. The results revealed that 14,542 pixels (53.89%) simultaneously satisfied the criteria for both DD and DTA. Additionally, 6,904 pixels (25.58%) failed only the DD criterion, while 1,075 pixels (3.98%) failed only the DTA criterion. Furthermore, 4,464 pixels (16.54%) failed to meet both criteria.

### 3.5. Comparison of Gamma Algorithms

Each algorithm exhibited distinct characteristics under different parameter thresholds. At stricter conditions (1%/1 mm), the Ju *et al.* algorithm showed a higher passing rate (55.14%) compared to the Low *et al.* method (21.78%). However, with relaxed thresholds (7%/7 mm), all algorithms converged to a 100% passing rate.

### 3.6. Impact of Parameter Variation (DTA and DD)

The sensitivity of gamma passing rates to variations in DD and DTA thresholds was systematically evaluated. At 1%/1 mm, the gamma passing rate for the Low *et al.* algorithm was 21.78%, while it reached 95.29% at 3%/3 mm and 100% at 7%/7 mm. Similar trends were observed for other algorithms, indicating that increasing the threshold consistently improves passing rates but may compromise the physical accuracy of the dose distribution (Figure 10, Table 2).

## 4. Discussion

The gamma index results demonstrated the robustness and accuracy of the IMRT treatment plan for laryngeal cancer. Under standard conditions (3%/3 mm), the high passing rate (95.29%) confirms the suitability of the treatment plan for clinical application. However, stricter thresholds (1%/1 mm) revealed limitations, highlighting areas for

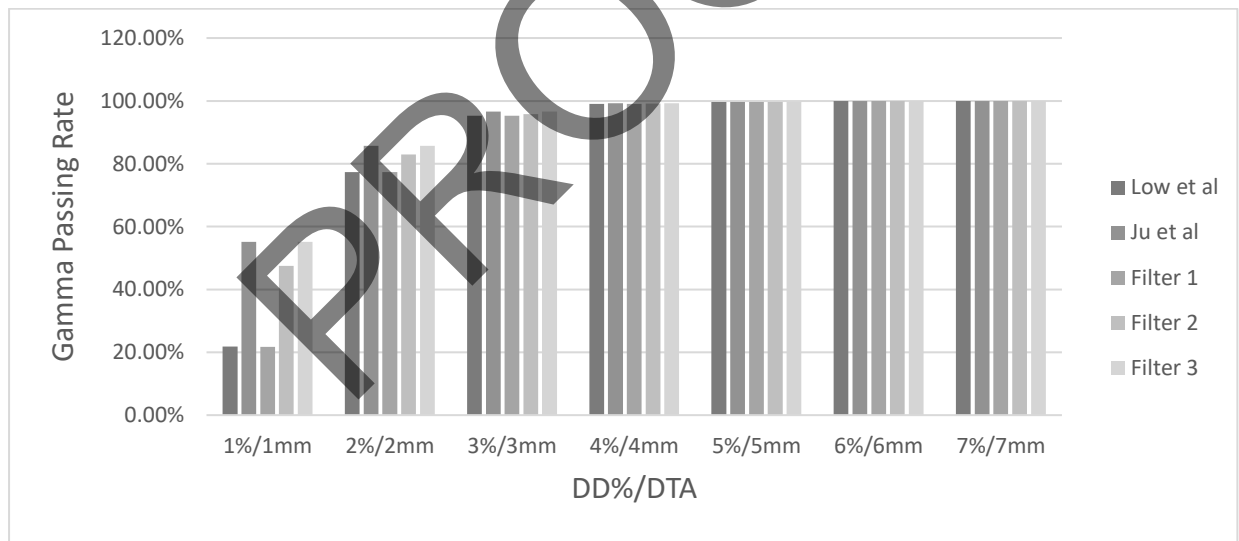


**Figure 10.** Bar chart showing the impact of different gamma calculation algorithms on gamma passing rates for the laryngeal IMRT plan

**Table 2.** Impact of different gamma calculation algorithms on gamma passing rates for the laryngeal IMRT plan

DD(%) / DTA(mm) Threshold	Low et al	Ju et al	Filter 1	Filter 2	Filter 3
1%/1mm	21.78%	55.14%	21.73%	47.51%	55.14%
2%/2mm	77.35%	85.71%	77.33%	82.93%	85.71%
3%/3mm	95.29%	96.63%	95.29%	95.83%	96.63%
4%/4mm	99.05%	99.22%	99.05%	99.16%	99.22%
5%/5mm	99.66%	99.68%	99.66%	99.67%	99.68%
6%/6mm	100%	100%	100%	100%	100%
7%/7mm	100%	100%	100%	100%	100%



optimization in dose delivery. The profile analysis indicated better agreement in the horizontal axis than the vertical axis, suggesting potential challenges in achieving uniform dose coverage in certain directions. Subtraction analysis further emphasized the need for improvement in low-dose regions, as a significant percentage of pixels exceeded the tolerance range. The subtraction and composite analyses provided deeper insights into dose distribution accuracy, complementing the gamma index evaluation. The subtraction plot highlighted localized dose discrepancies, while the composite analysis revealed the interplay between dose difference and distance-to-agreement criteria. These indicate that while the gamma index provides a general overview of dose agreement, the subtraction and composite analyses are more sensitive to localized discrepancies. This sensitivity can guide adjustments in treatment planning, ensuring more precise dose delivery, and minimizing the risk of underdosing or overdosing in critical areas. This highlights their value in fine-tuning and validating treatment plans for improved clinical outcomes.

In the study by Casanova Borca *et al.*, the dosimetric properties of Gafchromic EBT3 film for IMRT dose verification were evaluated. The results showed that EBT3 eliminates the orientation dependence seen in previous EBT2 films, making it suitable for clinical use [14].

In the study by Abedi Firouzjah *et al.*, the dosimetric accuracy of the Eclipse<sup>TM</sup> TPS was evaluated using EBT3 film and Delta4 in a heterogeneous chest phantom with the IMRT technique. The results showed that the gamma index passing rates for the film and Delta4 measurements were above 95%, indicating that Eclipse<sup>TM</sup> TPS provides accurate dose calculations within standard criteria [15].

In the study by Varsha R Gedam *et al.*, PSQA was conducted using Gafchromic EBT3 film for complex head, neck, and brain cancer treatments. The results showed that the GPR for both types of cases exceeded 95% with 3%/3 mm criteria, confirming that EBT3 film provides reliable dosimetric verification similar to 2D array systems [16].

In the study by Nalbant *et al.*, pre-treatment dosimetric verification of prostate IMRT plans was

performed using Gafchromic EBT3 film and 2D-Array. The results showed that both methods achieved over 90% compatibility with the TPS data using 3%/3 mm gamma criteria, with 2D-Array measurements being statistically closer to the TPS data. The study concluded that 2D-Array may be preferred for routine use due to its accuracy and shorter measurement time, while the 3%/3 mm gamma criteria were found to be the most suitable for IMRT quality assurance [17].

In the study by Rooshenass *et al.*, the accuracy of three dose calculation algorithms (ACUROSE XB, AAA, and PBC) in the Eclipse<sup>TM</sup> Treatment Planning System was compared using a heterogeneous phantom. The results showed that the ACUROSE XB algorithm provided the most accurate dose prediction in heterogeneous tissues like the lung, with maximum differences of 2.5%, 8.6%, and 16.1% for the AXB, AAA, and PBC algorithms, respectively. This highlights the superior performance of the AXB algorithm for dose calculations in complex tissue types [18].

In the study by Falahati *et al.*, the feasibility of using Gafchromic EBT3 film for dosimetric verification of IMRT plans in lung cancer treatment was evaluated. The IMRT plans were generated using the Prowess Panther TPS and compared with the measured doses from the EBT3 film placed in an inhomogeneity phantom. The study demonstrated that the gamma passing rates for various dose differences and distance to agreement criteria (3%/3mm, 4%/4mm, 5%/5mm, etc.) increased with broader criteria, indicating that EBT3 film is an effective tool for verifying IMRT treatment plans in clinical settings [19].

The comparison of gamma algorithms highlighted the variability in performance, particularly under stricter conditions. The Ju *et al.* algorithm consistently outperformed the Low *et al.* method for tighter thresholds, suggesting its potential suitability for cases requiring higher sensitivity. However, at relaxed thresholds, all algorithms demonstrated similar results. The findings underscore the importance of carefully selecting gamma analysis parameters to balance clinical relevance and dosimetric accuracy. Future studies should explore these evaluations for modern techniques such as VMAT and TomoTherapy to generalize the findings and further improve treatment quality assurance protocols.

## 5. Conclusion

This study demonstrated the feasibility of patient-specific quality assurance using gamma analysis for IMRT plans in laryngeal cancer, highlighting its ability to ensure treatment accuracy. The gamma analysis approach provides clinical physicists with a robust tool for verifying treatment plans. The use of different treatment algorithms indicates that, under the relaxed conditions, all algorithms perform similarly. However, under more stringent conditions, the JU *et al.* algorithm aligns with the third-filter algorithm proposed by Deputy *et al.*, with the key difference being that the former operates at a much faster speed. Despite the speed difference, the accuracy of both algorithms is comparable. The second algorithm relies heavily on numerous interpolation methods, suggesting that algorithms based on geometric response could provide high-speed performance while maintaining high accuracy for gamma analysis.

## References

- 1- S. A. Bhide, K. L. Newbold, K. J. Harrington, and C. M. Nutting, "Clinical evaluation of intensity-modulated radiotherapy for head and neck cancers." (in eng), *Br J Radiol*, Vol. 85 (No. 1013), pp. 487-94, May (2012).
- 2- M. E. Gamez, A. Blakaj, W. Zoller, M. Bonomi, and D. M. Blakaj, "Emerging Concepts and Novel Strategies in Radiation Therapy for Laryngeal Cancer Management." (in eng), *Cancers (Basel)*, Vol. 12 (No. 6), Jun 22 (2020).
- 3- M. A. Samuels, L. M. Freedman, and N. Elsayyad, "Intensity-modulated radiotherapy for early glottic cancer: transition to a new standard of care?" (in eng), *Future Oncol*, Vol. 12 (No. 22), pp. 2615-30, Nov (2016).
- 4- M. S. Swanson, G. Low, U. K. Sinha, and N. Kokot, "Transoral surgery vs intensity-modulated radiotherapy for early supraglottic cancer: a systematic review." (in eng), *Curr Opin Otolaryngol Head Neck Surg*, Vol. 25 (No. 2), pp. 133-41, Apr (2017).
- 5- Keyvan Jabbari, Alireza Amouheidari, and Shadi Babazadeh, "The Quality Control of Intensity Modulated Radiation Therapy (IMRT) for ONCOR Siemens Linear Accelerators Using Film Dosimetry." (in en), *Iranian Journal of Medical Physics*, Vol. 9 (No. 2), pp. 111-25, (2012).
- 6- G. A. Ezzell *et al.*, "Guidance document on delivery, treatment planning, and clinical implementation of IMRT: report of the IMRT Subcommittee of the AAPM Radiation Therapy Committee." (in eng), *Med Phys*, Vol. 30 (No. 8), pp. 2089-115, Aug (2003).
- 7- M. Miften *et al.*, "Tolerance limits and methodologies for IMRT measurement-based verification QA: Recommendations of AAPM Task Group No. 218." (in eng), *Med Phys*, Vol. 45 (No. 4), pp. e53-e83, Apr (2018).
- 8- M. Hussein, P. Rowshanfarzad, M. A. Ebert, A. Nisbet, and C. H. Clark, "A comparison of the gamma index analysis in various commercial IMRT/VMAT QA systems." (in eng), *Radiother Oncol*, Vol. 109 (No. 3), pp. 370-6, Dec (2013).
- 9- D. A. Low, W. B. Harms, S. Mutic, and J. A. Purdy, "A technique for the quantitative evaluation of dose distributions." (in eng), *Med Phys*, Vol. 25 (No. 5), pp. 656-61, May (1998).
- 10- L. Coleman and C. Skourou, "Sensitivity of volumetric modulated arc therapy patient specific QA results to multileaf collimator errors and correlation to dose volume histogram based metrics." (in eng), *Med Phys*, Vol. 40 (No. 11), p. 111715, Nov (2013).
- 11- J. H. Song *et al.*, "Gamma analysis dependence on specified low-dose thresholds for VMAT QA." (in eng), *J Appl Clin Med Phys*, Vol. 16 (No. 6), pp. 263-72, Nov 8 (2015).
- 12- T. Ju, T. Simpson, J. O. Deasy, and D. A. Low, "Geometric interpretation of the gamma dose distribution comparison technique: interpolation-free calculation." (in eng), *Med Phys*, Vol. 35 (No. 3), pp. 879-87, Mar (2008).
- 13- T. Depuydt, A. Van Esch, and D. P. Huyskens, "A quantitative evaluation of IMRT dose distributions: refinement and clinical assessment of the gamma evaluation." (in eng), *Radiother Oncol*, Vol. 62 (No. 3), pp. 309-19, Mar (2002).
- 14- V. Casanova Borca *et al.*, "Dosimetric characterization and use of GAFCHROMIC EBT3 film for IMRT dose verification." (in eng), *J Appl Clin Med Phys*, Vol. 14 (No. 2), p. 4111, Mar 4 (2013).
- 15- R. Abedi Firouzjah, A. Nickfarjam, M. Bakhshandeh, and B. Farhood, "The use of EBT3 film and Delta4 for the dosimetric verification of Eclipse<sup>TM</sup> treatment planning system in a heterogeneous chest phantom: an IMRT technique." (in eng), *International Journal of Radiation Research*, Technical Note Vol. 17 (No. 2), pp. 355-61, (2019).
- 16- V. R. Gedam and A. Pradhan, "EVALUATION OF PATIENT-SPECIFIC IMRT QUALITY ASSURANCE AND POINT DOSE MEASUREMENT FOR COMPLEX HEAD AND NECK AND BRAIN CANCER USING GAFCHROMIC EBT3 FILM." (in eng), *Radiat Prot Dosimetry*, Vol. 199 (No. 2), pp. 164-70, Feb 15 (2023).
- 17- Nalbant Nalbant, N DonmezKesen, and Bilge Hatice, "Pre-Treatment Dose Verification of Imrt Using

Gafchromic Ebt3 Film and 2DArray." *Journal of Nuclear Medicine and Radiation Therapy*, Vol. 5pp. 1-6, (2014).

- 18- Rooshenass Raheleh, Barough Mehdi Salehi, Gholami Somayeh, and Mohammadi Ehsan, "Dosimetric Accuracy Comparison between ACUROSE XB, AAA and PBC Dose Calculation Algorithms in Eclipse™ TPS Using a Heterogeneous Phantom." *Frontiers in Biomedical Technologies*, Vol. 6 (No. 4), 12/30 (2018).
- 19- F. Falahati, A. Nickfarjam, and M. Shabani, "A Feasibility Study of IMRT of Lung Cancer Using Gafchromic EBT3 Film." (in eng), *J Biomed Phys Eng*, Vol. 8 (No. 4), pp. 347-56, Dec (2018).

PROOF